Available online at www.sciencedirect.com
SCIENCE DIRECT
Synthetic Metals 155 (2005) 250–253
SYNTHETIC METALS
www.elsevier.com/locate/synmet

Excitons in semiconducting single-walled carbon nanotubes

Hongbo Zhao, Sumit Mazumdar*

Department of Physics, University of Arizona, Tucson, AZ 85721, USA

Received 4 January 2005; accepted 8 January 2005
Available online 27 October 2005

Abstract

We report correlated-electron calculations of optically excited states in 10 semiconducting single-walled carbon nanotubes with a wide range of diameters. Optical excitation occurs to excitons whose binding energies decrease with the increasing nanotube diameter, and are smaller than the binding energy of an isolated strand of poly-(paraphenylene vinylene). The ratio of the energy of the second optical exciton polarized along the nanotube axis to that of the lowest exciton is smaller than the value predicted within single-particle theory. The experimentally observed weak photoluminescence is an intrinsic feature of semiconducting nanotubes, and is consequence of dipole-forbidden excitons occurring below the optical exciton. Excited states absorption calculations show photoinduced absorption energies are lower than or comparable to the binding energy of the lowest exciton.

Keywords: Carbon nanotubes; Semiempirical models and model calculations; Photoluminescence

1. Introduction

Recent experiments in semiconducting single-walled carbon nanotubes (SWCNTs) have indicated the strong role of electron–electron (e–e) interactions [1–5], ignored in one-electron theories [6]. Several observations have attracted particular attention. First, optical gaps in SWCNTs are considerably greater [1–3] than those predicted from the tight-binding (TB) model [6]. Second, the ratio of the threshold energy corresponding to the second optical transition (E_{22}) polarized along the SWCNT axis to that of the first such transition (E_{11}) is less than the value two [2–4] predicted within the TB model for wide SWCNTs [6]. It has been claimed that this "ratio problem" is a signature of e–e interactions [7–9]. Third, ultrafast pump–probe spectroscopy [5] has revealed *structured* photoinduced absorptions (PA) and correlations of PA with photoinduced bleaching (PB), that indicate that photoexcitations in SWCNTs are excitons. These observations have led to theoretical studies of SWCNTs that go beyond one-electron models [7–14]. Different calculations have, however, focused on different approaches and often on specific SWCNTs, and while a consensus is emerging that optical absorptions in semiconducting SWCNTs are due to excitons, complete physical understanding of the generic effects of e–e interactions is still missing.

In the present paper, we investigate SWCNTs within the semiempirical Pariser–Parr–Pople (PPP) π-electron Hamiltonian [15,16] that has been used extensively to discuss π-conjugated polymers [17–23], which exhibit strong excitonic features [24–28]. The advantages of the semiempirical approach are: (i) immediate connection to the rich physics of π-conjugated polymers can be made and (ii) the dominant effects of e–e interactions in SWCNTs can be understood physically.

2. Theoretical model

We consider the PPP model Hamiltonian [15,16]

$$H = H_{1e} + H_{e\text{–}e}$$

where H_{1e} is the one-electron Hückel Hamiltonian and $H_{e\text{–}e}$ is the e–e interaction,

$$\begin{aligned} H_{1e} &= -t\sum_{\langle ij\rangle,\sigma} c^{\dagger}_{i,\sigma}c_{j,\sigma} + \text{H.c.} \\ H_{e\text{–}e} &= U\sum_{i} n_{i,\uparrow}n_{i,\downarrow} + \frac{1}{2}\sum_{i,j} V_{ij}(n_i - 1)(n_j - 1) \end{aligned} \tag{1}$$

* Corresponding author. Tel.: +1 520 621 6803; fax: +1 520 621 4721.
E-mail address: sumit@physics.arizona.edu (S. Mazumdar).

0379-6779/$ – see front matter © 2005 Elsevier B.V. All rights reserved.
doi:10.1016/j.synthmet.2005.01.029

Here, $c^{\dagger}_{i,\sigma}$ creates a π-electron of spin σ on carbon (C) atom i, $\langle ij\rangle$ indicates nearest neighbors and $n_i = \sum_\sigma c^{\dagger}_{i,\sigma} c_{i,\sigma}$ is the total number of π-electrons on site i. The parameters t, U and V_{ij} are the nearest neighbor hopping integral, the on-site and intersite Coulomb interactions, respectively. We have chosen the standard value of 2.4 eV for t [17–22]. Our parameterization of long-range V_{ij} is similar to the standard Ohno parameterization [29]

$$V_{ij} = \frac{U}{\kappa\sqrt{1 + 0.6117R_{ij}^2}}$$

where R_{ij} is the distance between C atoms i and j in Å, and κ is a screening parameter ($\kappa = 1$ within Ohno parameterization) [30]. We have done calculations for $U/t = 1.9$, 2.5, 3.33 and 4.0, and $\kappa = 1$ and 2, and our qualitative conclusions are similar for all cases. We report the results for only $U/t = 3.33$ and $\kappa = 2$, since this combination was found to be the most suitable for PPV [30], and it is likely that the Coulomb parameters in phenyl-based π-conjugated polymers and SWCNTs are similar.

Full many-body calculation within Eq. (1) is not possible for SWCNTs. We use the single configuration interaction (SCI) approximation [17–19,23,30], which is a many-body approach valid within the subspace of single excitations from the Hartree–Fock (H–F) ground state. While SCI is not sufficient for two-photon states, semiquantitative results are obtained for one-photon states.

We use open boundary condition along the nanotube (NT) axis, such that evaluations of transition dipole matrix elements are simple. Surface states originating from ends of open tubes can be detected from their energies at the chemical potential in the $U = V_{ij} = 0$ Hückel limit and their one-electron wave functions, and they are excluded from the SCI calculations. We have performed calculations for seven semiconducting zigzag (n, 0) NTs for n ranging from 7 to 17, and (6, 2), (6, 4) and (7, 6) chiral NTs. The number of unit cells N in SCI calculations for zigzag NTs is 18. For the chiral NTs with large unit cells, we determined from Hückel calculations the N at which infinite system absorption thresholds are reached, and performed the SCI calculations for these N. Our calculations are for $N = 10$, 8 and 2 in the (6, 2), (6, 4) and (7, 6) NTs, with 1040, 1216 and 1016 C atoms, respectively.

3. Results and discussion

We begin our discussions with the lowest energy excitations. In the zigzag SWCNTs, the highest valence band (v.b.) and lowest conduction band (c.b.) for $H_{e\text{–}e} = 0$ are doubly degenerate [6]. In the chiral SWCNTs, the degenerate levels occur at different single-particle crystal momenta [6]. Nevertheless, in both cases there occur doubly degenerate single-particle excitations with total crystal momentum zero.

Consider now the four degenerate lowest single-particle excitations in SWCNTs, $\chi_{a\to a'}$, $\chi_{a\to b'}$, $\chi_{b\to a'}$ and $\chi_{b\to b'}$, shown in Fig. 1, where a and b (a′ and b′) are the highest occupied (lowest unoccupied) one-electron levels. The two excitations $\chi_{a\to a'}$ and $\chi_{b\to b'}$ are optically allowed, and for non-zero matrix elements of $H_{e\text{–}e}$ between them, new non-degenerate eigenstates

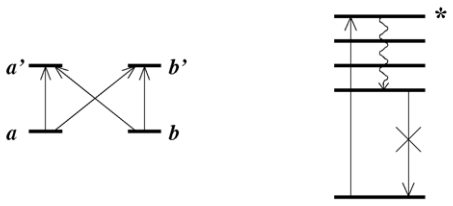

Fig. 1. Left: schematic of the four degenerate single-particle excitations from the highest occupied to the lowest unoccupied one-electron levels in SWCNTs. Right: these degeneracies are split by $H_{e\text{–}e}$, and only the highest state (marked with *) is strongly dipole-allowed. Rapid relaxation occurs to the lowest forbidden exciton, radiative relaxation from which is forbidden.

$\chi_{a\to a'} \pm \chi_{b\to b'}$ are obtained. There also occur superpositions involving the dipole-forbidden excitations, as well as others involving immediately lower v.b. and higher c.b. levels. Significantly, (i) the odd superposition is dipole forbidden and (ii) for repulsive $H_{e\text{–}e}$ the allowed even superposition is higher in energy, as is indicated in Fig. 1. In Table 1, we have listed (n, m) for all the SWCNTs we have investigated, and the corresponding differences in total energies δE between the optically allowed exciton and the lowest exciton.

The low QE of PL ($<10^{-3}$) [4,31–33] in SWCNTs is an intrinsic feature of isolated NTs, and not a consequence of exciton quenching. As shown in Table 1, $\delta E \sim 3$–$4k_BT$. Thus, following the rapid relaxation into the forbidden lowest exciton it is unlikely that thermal effects will re-excite the system to the allowed state. Intrinsic radiative decay rate therefore should be low, and the radiative lifetimes long. Simultaneously, δE is small enough that small amounts of impurities or changes in the environment can modify the emissive behavior. This may explain the strong dependence of the emission on the environment [4,31,33,34]. Recent estimates of very long exciton lifetimes [32,33] are in agreement with our work. Femtosecond time-resolved measurements indicate same decay rates for fluorescence and PB, but the PB drops to only half its peak value [33]. We agree with Ref. [33] that this is an indication of trapping of the excitation in a non-emissive state. We also believe that the non-emissive state is the forbidden exciton found here.

Within TB theory, interband excitations responsible for optical absorptions polarized transverse to the tube axis, $\chi_{1\to 2'}$ and $\chi_{2\to 1'}$ (see inset, Fig. 2), are also degenerate. As shown elsewhere [8,17–19], e–e interaction will also split these excitations.

Table 1
Summary of computed SCI results for different SWCNTs

(n, m)	d (Å)	δE (eV)	E_{b1} (eV)	E_{b2} (eV)	E_{22}/E_{11}
(7, 0)	5.56	0.11	0.54	0.78	1.80
(6, 2)	5.72	0.062	0.53	0.72	1.82
(8, 0)	6.35	0.098	0.53	0.58	1.67
(6, 4)	6.92	0.057	0.48	0.55	1.72
(10, 0)	7.94	0.13	0.41	0.57	1.65
(11, 0)	8.73	0.092	0.42	0.45	1.73
(7, 6)	8.95	0.073	0.37	0.47	1.68
(13, 0)	10.3	0.11	0.32	0.45	1.58
(14, 0)	11.1	0.089	0.34	0.39	1.68
(17, 0)	13.5	0.086	0.29	0.31	1.70